Numerical simulation of the gas diffusion process during an air ingress accident in the HTR-PM

ZUO Hong-wei[1], DONG Yu-jie[2], and LIU Bao-ting[3]

1. State Nuclear Power Engineering Company, Shanghai, 200233 China (zuohongwei@snpec.com.cn)
2. Institute of Nuclear and New Energy Technology, Tsinghua University, Beijing, 100084 China
3. China Nuclear Power Design Co., Ltd, Shanghai Branch, Shanghai, 200030 China

Abstract: The consequence of an air ingress accident can be greatly influenced by the gas-diffusion process. It is necessary to study the process of air diffusion in the cavity of the reactor through the rupture of hot gas ducts of the High Temperature Gas-cooled Reactor Pebble-bed Module (HTR-PM) until steady convection forms. The DIFFLOW code was used for the numerical simulation that illustrated the gas-diffusion process inside of the HTR-PM. In the sensitivity analysis, the core temperature, the diffusion coefficient, the frictional resistance coefficient and the surface coefficient of heat transfer proved to be the impact factors. Each factor was evaluated with three levels. The onset time of the steady convection, the velocity in the middle passage under steady convection, and the mass flow in the middle passage under steady convection were observed in the analysis. 32.78 hours after the accident occurs, the steady convection could be established. The flow in the middle passage under steady convection measured 0.32kg/s, while the velocity in the middle passage read 0.56m/s. The sensitivity analysis also showed that the core temperature had a remarkable impact on the onset time, the velocity and the flow of the steady convection.
Keyword: HTR-PM; air ingress accident; gas diffusion

1 Introduction

The High Temperature Gas-cooled Reactor Pebble-bed Module (HTR-PM) has qualities that guarantee its inherent safety, high generating efficiency, and versatile utilization. It is widely accepted that the HTR-PM is a new kind of reactor integrating the main features of Generation IV reactors.

The HTR-PM plant consists of two nuclear steam supply systems (NSSS), so called modules, each one comprising a single zone 250MWth pebble-bed modular reactor and a steam generator. The two NSSS modules feed one steam turbine and generate an electric power of 210MW. The reactor and the steam generator are installed inside two separate pressure vessels. The pressure vessels are assembled in a staggered, side-by-side arrangement and are connected by a horizontal coaxial hot gas duct. The primary pressure boundary consists of the reactor pressure vessel (RPV), the steam generator pressure vessel (SGPV) and the hot gas duct pressure vessel (HDPV), which are all housed in a concrete shielding cavity. The main helium blower is mounted on the upper part of the steam generator pressure vessel. The core inlet helium temperature operates at 250℃ while the outlet helium temperature reaches 750℃. The blower transfers helium, which serves as mediator to conduct the heat of the reactor to the steam generator, where high-pressure superheated steam is produced which drives the steam turbine. [1] Design specifications of the HTR-PM are shown in Table 1. The flow diagram of the HTR-PM is shown in Fig.1.

Table 1 Design specifications of the HTR-PM

Parameters	Design value
Reactor power, MW(th)	250
Active core diameter, m	3.0
Active core height, m	11.0
Reactor pressure vessel inside diameter, mm	5700
Helium pressure of primary loop, MPa	7.0
Inlet/outlet helium temperature, ℃	250/750
Number of fuel elements in equilibrium core	420,000
Main feed-water temperature, ℃	205
Main steam temperature, ℃	571
Main steam pressure, MPa	13.9
Feed-water flow rate for one reactor steam generator, kg/s	98
Inner/outer diameter of the annular channel of the coaxial duct, mm	1030/1565
Diameter of the central tube of the coaxial duct, mm	750

Received date: August 4, 2010
Revised date: May 3, 2011

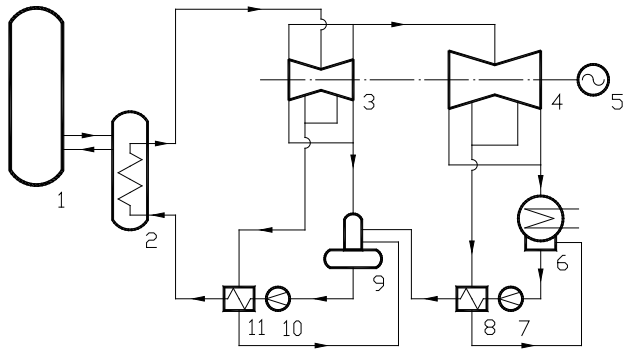

1.Reactor; 2. Steam generator; 3.High pressure turbine;
4.Low pressure turbine; 5.Generator; 6.Condenser;
7. Condensate pump; 8.Low pressure feedwater heater;
9.Deaerator; 10.Feedwater pump;
11.High pressure feedwater heater

Fig. 1 HTR-PM plant diagram.

A standardized module can be easily constructed in real scale. The relatively small nuclear power-output of a reactor module is flexible enough to meet market requirements.

The gas-diffusion process happening during an accident involving the rupture of a hot gas duct of the HTR-PM is described in this paper. The study aims to provide the theoretical basis for the validation of the inherent safety features of the HTR-PM.

2 Description of the primary circuit

Under normal operation, the coolant of the HTR-PM, which is pumped by the helium blower, flows sequentially through the annular channel of the coaxial duct, the inlet of coolant, and finally the cool helium plenum . In the plenum that is situated at the bottom of the reactor pressure vessel, the direction of the flow changes. After having cooled the fuel elements in the discharging tube, a minute amount of the coolant is collected in the hot helium plenum. A large amount of the coolant flows into the top cold helium plenum vying the passage in the side graphite reflector. Then a minute of this helium flows through the control rod channels to lower their temperature. A large amount of helium is distributed to the channels of the top reflector. This part of coolant flows down through the pebble-bed core to bring the decay heat out. Heated helium is collected into the hot helium plenum. Then the heated helium flows into the steam generator through the central tube of the coaxial duct. After exchanging heat with the cooling water, the coolant is sucked into the blower again. This process is referred to as the helium circulation of the primary circuit. The primary circuit of the HTR-PM is shown in Fig. 2.

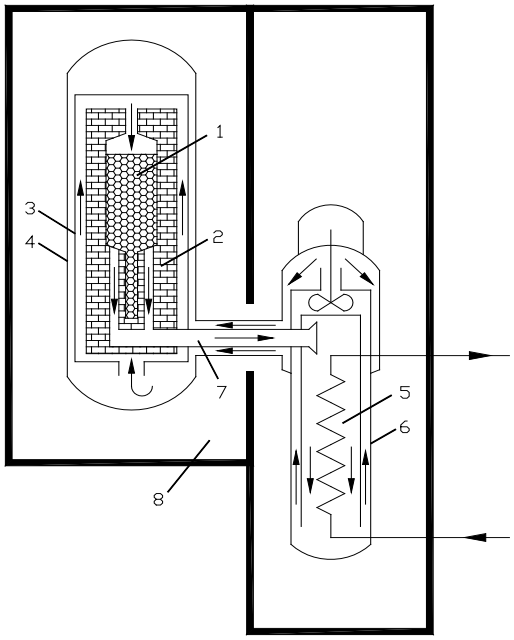

1.Reactor core; 2.Graphite reflector; 3.Core barrel; 4.Reactor pressure vessel; 5.Steam generator; 6.Steam generator vessel; 7.Coaxial gas duct; 8.Cavity

Fig. 2 Cross section of the primary circuit of HTR-PM.

3 Accident process

The rupture of the connection pipe between the reactor pressure vessel and the steam generator pressure vessel can cause an air ingress accident, even if there is a fairly low possibility that it occurs. Although the penetrations through reactor pressure vessel will be designed to withstand a safe shutdown, in case of earthquake, which represents an event beyond design considerations, it is conservatively assumed that the residual stress can cause the core outlet pipe to break.[1] During an air ingress accident, high pressure helium in the primary circuit leaks into the cavity due to the rupture. Then the air pressure of the cavity, which approximately equals to local atmosphere pressure in normal operation conditions, rises until it reaches 0.11MPa, the pressure at which a safety discharge of the cavity occurs. After the

discharge, the pressure of the cavity and the primary circuit is equal to the pressure of the atmosphere. Air in the cavity diffuses into the reactor slowly because the density of air is higher than that of helium. Convection commences after adequate diffusion. The difference of temperature impels the convection, which flows up through the pebble-bed and flows down through the side reflector passage. Even though the convection is weak, the graphite can be corroded by air during a long period. [2, 3] Therefore, research on the gas-diffusion process is a prerequisite to the understanding of the graphite corrosion process. In this paper, the scope of the study does not involve the graphite corrosion process.

4 Calculation model

The passage structure of the HTR-PM includes different sectors which have diverse hydraulic features. For example, the pebble-bed, the helium plenum, the reflector passages, the chambers and so on are all different in this aspect. It seemed beneficial to simplify the passage in the calculation process. The pebble-bed was proposed to be uniform porous media with a porosity of 0.39. The annular channel of the coaxial duct was simplified into a pipe. The passages in the side reflector, top reflector and bottom reflector were also replaced with pipes. Fuel elements in the discharge tube require cooling helium. The flow in the discharge tube was neglected as it was a minute amount. At the same time, the cooling flow in the control rods channels, which carries the heat while the control rods absorb neutrons, was ignored. The flow through the steams between graphite bricks was negligible. The bypass flows mentioned above account for about 10% of the total flows. The delaying function of some chambers in the reactor was neglected. Nitrogen was the largest component of air. At the same time, we relied on diffusion coefficients available for three or more sorts of gases based on accurate experimental measurements. Only nitrogen and helium were taken into account during the numerical simulation process. The primary circuit model based on the simplified HTR-PM channels is shown in Fig. 3.

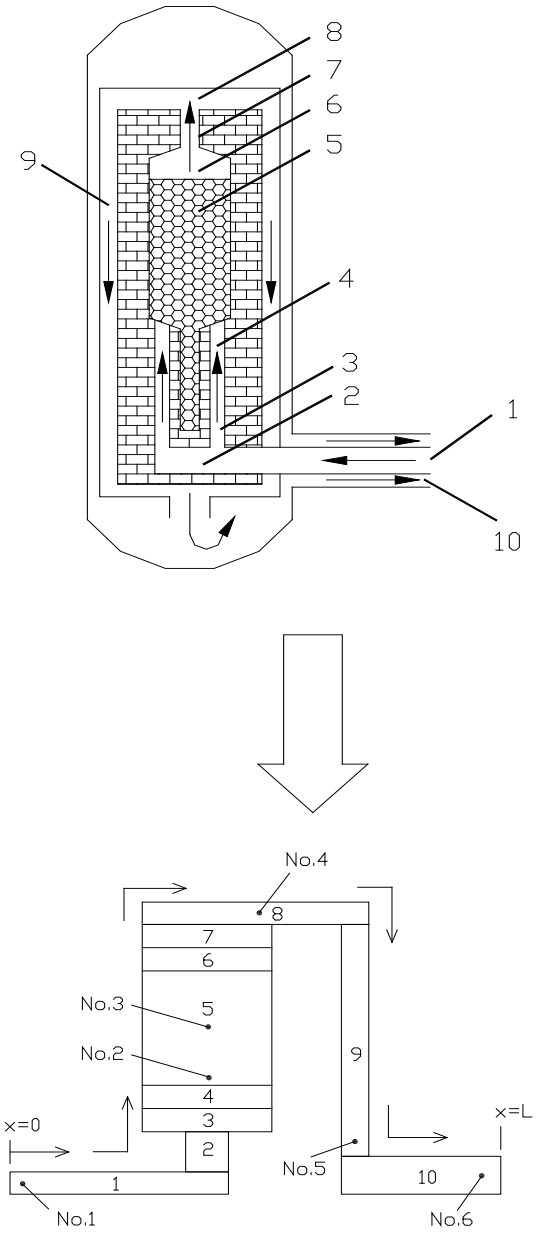

1.Central tube of coaxial duct; 2.Hot helium plenum; 3.Bottom reflector channel (lower); 4.Bottom reflector channel (upper); 5.Pebble-bed; 6.Top chamber; 7. Top reflector channel; 8.Cold helium plenum; 9.Side reflector channel; 10.Annular channel of coaxial duct

Fig. 3 Diffusion-convection model of The primary circuit of the HTR-PM.

5 Computing code

The DIFFLOW code[2] was taken advantage of to simulate the diffusion process. The code can accurately simulate the process of a diffusion experiment held at the Japan Atom Energy Research Institute (JAERI). JAERI's diffusion experiment device is shown in Fig. 4. This device is an experimental facility used to analyze the air ingress into a HTTR reactor. The diffusion in the early stage of an air ingress accident at the high temperature gas cooled reactor has been studied by M. Hishida of JAERI in the frame of the Japanese HTTR program.

An experiment in a reverse-U-shaped tube has been carried out and a one-dimensional coupled diffusion-convection model has been established. The hot leg simulates the reactor core and the cold leg simulates the annular channel between the core vessel and the reactor pressure vessel. The temperatures of the tube were controlled as being nearly constant during the experiment. Nitrogen was used to simulate air and the chemical reactions in the reactor were not considered. [3, 4]

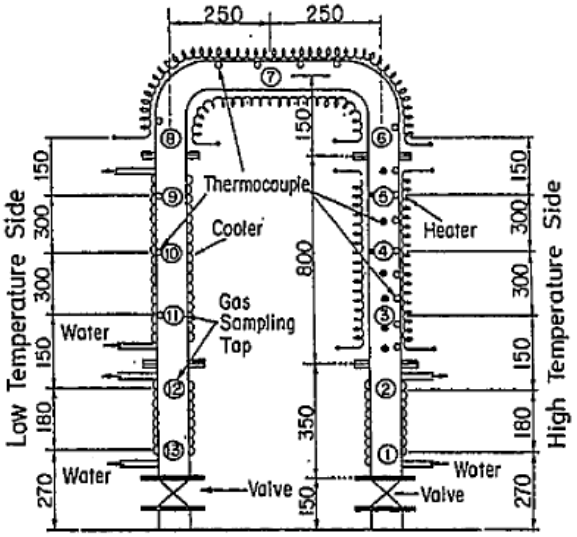

Fig. 4 JAERI's diffusion experiment device.

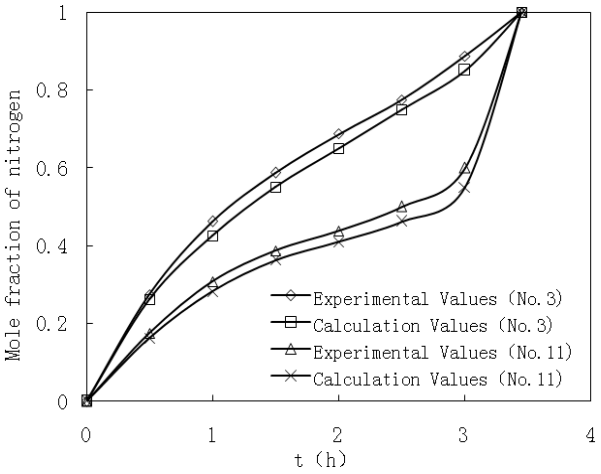

Fig. 5 Comparison between the experiment and calculations using the DIFFLOW code.

A comparison between the experimental data and the calculation results of the DIFFLOW code is shown in Fig.5.[2] One-dimensional diverse-cross-area transient governing equations were used to describe the diffusion and convection in the code. The governing equations in the DIFFLOW code consist of a mass conservation equation

$$A\frac{\partial \rho}{\partial t}+\frac{\partial (A\rho u)}{\partial x}=0 \tag{1}$$

a momentum conservation equation

$$A\frac{\partial (\rho u)}{\partial t}+\frac{\partial (A\rho uu)}{\partial x}=-\rho g\xi A-r\frac{A}{D_H{}^2}u-\frac{\partial (pA)}{\partial x} \tag{2}$$

where $r=C_f\frac{\rho uD_H}{2}+K\frac{\rho uD_H{}^2}{2}$,

an energy conservation equation

$$A\frac{\partial (\rho c_pT)}{\partial t}+\frac{\partial (A\rho c_puT)}{\partial x}=\frac{\partial}{\partial x}(A\lambda\frac{\partial T}{\partial x})+q_{eff}A \tag{3}$$

a diffusion equation

$$A\frac{\partial (Cx_i)}{\partial t}+\frac{\partial}{\partial x}(AuCx_i)=\frac{\partial}{\partial x}(ACD_i\frac{\partial x_i}{\partial x}) \tag{4}$$

and the ideal gas law.

Initial and boundary conditions of pressure were

$p_a=10^5$Pa;
x=0, p=0Pa; x=L, p=0Pa. (5)

Initial and boundary conditions of velocity were

u=0m/s;
x=0, $\frac{\partial u}{\partial x}=0$; x=L, $\frac{\partial u}{\partial x}=0$. (6)

Initial and boundary conditions of temperature were

$T=T_W$;

$$x=0,\quad T=\begin{cases}T_\infty, u_0\ge 0;\\ \frac{\partial T}{\partial x}=0, u_0<0;\end{cases}$$

$$x=\text{L},\quad T=\begin{cases}T_\infty, u_L<0;\\ \frac{\partial T}{\partial x}=0, u_L\ge 0.\end{cases} \tag{7}$$

Initial and boundary conditions of concentration were

$$x_{N_2}^0=0;\ x_{He}^0=1;\quad x_{N_2}^\infty=1;\ x_{He}^\infty=0,$$

$$x=0,\quad x_i=\begin{cases}x_i^\infty, u_0\ge 0;\\ \frac{\partial x_i}{\partial x}=0, u_0<0;\end{cases}$$

$$x=\text{L},\quad x_i=\begin{cases}x_i^\infty, u_L<0;\\ \frac{\partial x_i}{\partial x}=0, u_L\ge 0.\end{cases} \tag{8}$$

The binary diffusion coefficient for nitrogen and helium was adopted as the most effective diffusion coefficient.

As to the discretization scheme of space terms in differential equations, the fully implicit scheme (*i.e.*, the values at the end of the time step) was adopted in the DIFFLOW code. A hybrid scheme was applied the discretization scheme for the discretization coefficients of convection-diffusion terms.

The discretization equation system can be solved by the TriDiagonal Matrix Algorithm (TDMA). The system containing momentum equations, pressure correction equations, energy equations and diffusion equations can be solved by the Semi-Implicit Method for Pressure Linked Equations Consistent (SIMPLEC). The general equation of momentum equations, pressure correction equations, energy equations and diffusion equations is

$$A_W \Phi_W + A_P \Phi_P + A_E \Phi_E = S \tag{9}$$

Where, A_W, A_P and A_E are the discretization coefficients on the left nodes, local nodes and right nodes, respectively. Φ_W, Φ_P, Φ_E are the values (*i.e.*, u, p', T, x_i) to be solved on the left nodes, local nodes and right nodes, respectively. S indicates the source terms.

Firstly, the coefficients (A_W, A_P and A_E) of the four equations are solved. By substitution of the coefficients and the original velocity field, pressure field, temperature field and concentration field in the general equation, we get the error, *i.e.*,

$$\varepsilon_\Phi = \max_{I=1}^{N}(A_{WI}\Phi_{WI} + A_{PI}\Phi_{PI} + A_{EI}P_{EI} - S_I) \tag{10}$$

When all the errors on all nodes meet the setting error, *i.e.*,

$$\max(\varepsilon_u, \varepsilon_p, \varepsilon_T, \varepsilon_{xi}) < \varepsilon \tag{11}$$

The iterative process can be accomplished for it is assumed to be convergent. Then the calculation can process to next time step. The calculation runs until steady convection forms. If the inequality above cannot be met, the iteration must continue. After the accident blowdown, the passage of the reactor is filled with helium. The cavity is filled with mixed gas of air and helium. For the sake of simplicity, the original conditions of the equations were assumed to be that the gas in the reactor channel was helium and the gas in the cavity was nitrogen. All gases were in a stationary state. The temperature of gases was equal to the temperature of channel walls. The time step was 1 second. Smaller time steps could obviously not affect the calculation results. The node distance was 0.55m. The node distance was decided based on the simulated temperature field. [5, 6]

6 Results and analysis

6.1 Results

The reactor would be scrammed and the helium blower would be stopped if the loss of cooling accident happened. Preliminary safety analysis indicates that, 0~26 hours after the loss of cooling, mean temperature of the fuel elements would keep rising. After about 26~28 hours after the loss of cooling, mean temperature of the fuel elements would reach its maximum value. [5, 6] The evaluation was performed with the THERMIX program. The core temperature distribution would just show minor changes during 26~50 hours after the beginning of the accident. T_W is the channel wall temperature after 28 hours of shutdown. This is the worst circumstance for the shortest onset time of steady convection can be formed in this condition. T_W kept constant during simulations. For higher temperature resulting into shorter steady convection onset time, using the constant temperature field is theoretically conservative. Six nodes in the model were chosen to be surveyed for their time-dependent nitrogen mole fraction, velocity and mass flow. Node no.1 was adjacent to the rupture of the central tube of the coaxial duct. Node no.2 was at the bottom of the core. Node no.3 was in the middle of the core. Node no.4 was in the middle of the whole passage. Node no.5 was situated at the bottom of the side reflector channel. Node no.6 was adjacent to the rupture point of the annular tube of the coaxial duct. The calculation results are shown in Figs. 6-13. The onset time of the steady convection, the velocity in the middle passage under steady convection and the mass

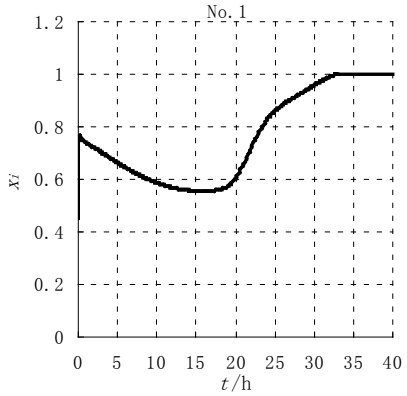

Fig. 6 Mole fraction of nitrogen on node No.1.

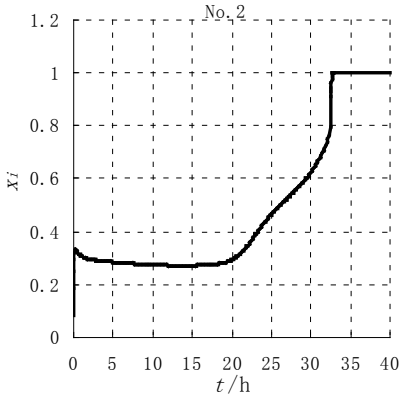

Fig. 7 Mole fraction of nitrogen on node No.2.

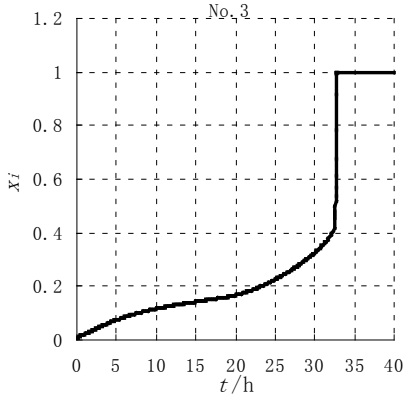

Fig. 8 Mole fraction of nitrogen on node No.3.

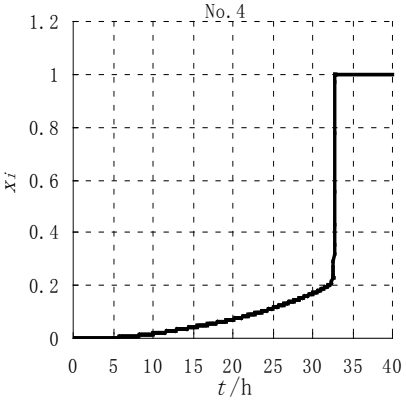

Fig. 9 Mole fraction of nitrogen on node No.4.

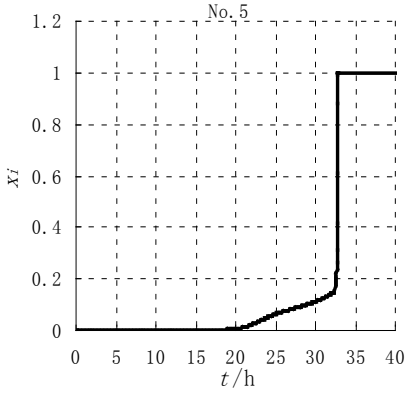

Fig. 10 Mole fraction of nitrogen on node No.5.

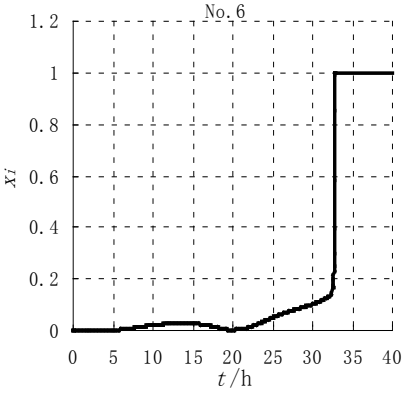

Fig. 11 Mole fraction of nitrogen on node No.6.

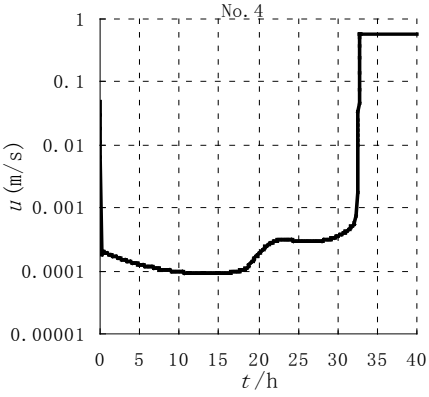

Fig. 12 Convection velocity on node No.4.

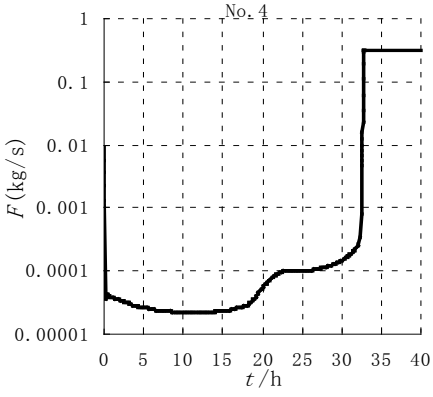

Fig. 13 Convection flow on node No.4.

Table 2 Orthogonal experiments and results

	T_W	D_i	C_f	α	t(h)	v(m/s)	F(kg/s)
1	95%(1)	95%(1)	95%(1)	95%(1)	40.69	0.581	0.331
2	95%(1)	100%(2)	100%(2)	100%(2)	38.72	0.557	0.323
3	95%(1)	105%(3)	105%(3)	105%(3)	36.95	0.534	0.315
4	100%(2)	95%(1)	100%(2)	105%(3)	34.48	0.561	0.316
5	100%(2)	100%(2)	105%(3)	95%(1)	32.83	0.548	0.307
6	100%(2)	105%(3)	95%(1)	100%(2)	31.20	0.586	0.324
7	105%(3)	95%(1)	105%(3)	100%(2)	29.44	0.550	0.300
8	105%(3)	100%(2)	95%(1)	105%(3)	27.90	0.589	0.316
9	105%(3)	105%(3)	100%(2)	95%(1)	26.64	0.574	0.307

Table 3 Analysis of the results of the experiment of the steady convection onset time (h)

	T_W	D_i	C_f	α
K_1	116.36	104.61	99.79	100.16
K_2	98.51	99.45	99.85	99.36
K_3	83.98	94.79	99.22	99.32
$\bar{K}_1$	38.79	34.87	33.26	33.39
$\bar{K}_2$	32.84	33.15	33.28	33.12
$\bar{K}_3$	27.99	31.60	33.07	33.11
R	10.80	3.27	0.21	0.28

Table 4 Analysis of the results of the experiment of steady convection velocity (m/s) in the middle passage

	T_W	D_i	C_f	α
K_1	1.673	1.693	1.756	1.704
K_2	1.695	1.694	1.692	1.693
K_3	1.713	1.695	1.633	1.684
$\bar{K}_1$	0.558	0.564	0.585	0.568
$\bar{K}_2$	0.565	0.565	0.564	0.564
$\bar{K}_3$	0.571	0.565	0.544	0.561
R	0.013	0.001	0.041	0.007

Table 5 Analysis of the results of the experiment of the steady convection mass flow rate (kg/s)

	T_W	D_i	C_f	α
K_1	0.969	0.947	0.972	0.946
K_2	0.947	0.946	0.946	0.947
K_3	0.924	0.946	0.922	0.947
$\bar{K}_1$	0.323	0.316	0.324	0.315
$\bar{K}_2$	0.316	0.315	0.315	0.316
$\bar{K}_3$	0.308	0.315	0.307	0.316
R	0.015	0.001	0.017	0.001

flow in the middle passage under steady convection were observed in the simulation. A mole fraction of nitrogen reaching 1 means that 100% of the helium is replaced by gas in the cavity. And it means the constant gas ingredients and gas flow can be formed then. It indicates that the steady convection is forming. In Figs. 6-13, we can see that 32.78 hours after the accident occurring, the steady convection can form.

That is to say, the mean temperature of the fuel elements reaches its maximum value about 28 hours after the loss of cooling, 4.78 hours after what, the steady convection forms.

Fig. 12 indicates that the velocity in the middle passage under steady convection reads 0.56m/s. The flow in the middle passage under steady convection measures 0.32kg/s, which is illustrated in Fig. 13. After the accident occurring, the pressure in the primary circuit quickly falls down to the level of the environment. The diffusion process commences after the blowdown. The convection tendency is strong for higher core temperature and lower side reflector channel temperature. The direction of the helium flow is from the rupture of the central tube of the coaxial duct to the core, then to the side reflector channel, and finally to the rupture of the annular tube of the coaxial duct. The air in the cavity flows into the reactor core following the helium flow. Then the convection tendency is reduced by the entrance of cooling air, whose density is greater than that of hot helium. Comparison between Fig.8 and Fig.10 shows that the mole fraction of air in the core increases faster than that in the side reflector channel. The lower convection tendency results in the smaller convection velocity and flow rate. For the velocity illustrated in Fig. 12, 250 seconds after the accident, the gas velocity in the middle passage reads 6.6mm/s, while the gas flows at 1.3g/s, as illustrated in Fig. 13. Then the gas velocity in the middle passage quickly falls to 0.18mm/s and the gas flow decreases to 0.037g/s in

500 seconds. This is the flow dropping phase. There are no obvious fluctuations of velocity and flow until 32.43 hours after the accident. At that time, the gas velocity in the middle passage is 1.7mm/s and the gas flow is 0.8g/s. This is the flow balancing phase. Beyond this time, the gas velocity quickly rises to 10mm/s and the gas flow increases to 4.6g/s in 500 seconds. This is the flow rising phase.

6.2 Sensitivity analysis

For measuring the impact of key parameters on the process of diffusion-convection, orthogonal experiments with four factors (*i.e.*, core temperature T_W, diffusion coefficient D_i, frictional resistance coefficient C_f and surface coefficient of heat transfer α) were designed. Each parameter had three levels (95% rating value, 100% rating value, 105% rating value). The reason motivating the choice of the four factors was their were use in calculation of the discretization coefficients and source terms of the discretization equation system. These experiments were intended to measure how much the four factors affect the onset time of steady convection, the steady convection velocity in the middle passage and the steady convection mass flow. The six nodes named No.1 to No.6 represent different parts of the fluid passage in reactor. The results on these six nodes indicated the development of diffusion during the experiments.

The experimental results on these six nodes can be seen in Table 2 to Table 5. In these tables, t is defined as the onset time of steady convection. v is defined as the velocity of steady convection. F is defined as the flow of steady convection. K_i is defined as the sum of all evaluation values on level i.

$\overline{K}_i$ is defined as the mean of all evaluation values on level i. R is defined as the range of means.

The sensitivity analysis shows that the core temperature has a remarkable impact on the onset time, the velocity and the flow of steady convection. From Table 3, we can see that when the range of temperature means is maximal, then that to the frictional resistance coefficient reaches its lowest value. So the dominant factors of the onset time of steady convection are the core temperature and the diffusion coefficient in turn. The higher core temperature and larger diffusion coefficient lead to shorter onset time. By comparing with each range of means, Table 4 and Table 5 indicate that the dominant factors of velocity and flow of steady convection are the frictional resistance coefficient and the core temperature. A smaller frictional resistance coefficient and a higher core temperature result in larger steady convection velocity. A smaller frictional resistance coefficient and a lower core temperature cause larger steady convection mass flow.

7 Conclusions

According to the flow conditions, the development of the diffusion-convection process can be divided into three stages: flow dropping, flow balancing, and flow rising. It can be concluded that the factors impacting the onset time of the steady convection are sequentially the core temperature, the diffusion coefficient, the surface coefficient of heat transfer, and the frictional resistance coefficient. The factors impacting the steady convection's velocity and mass flow in the middle passage are sequentially the frictional resistance coefficient, the core temperature, the surface coefficient of heat transfer, and the diffusion coefficient.

The simulation results show that 32.78 hours after the occurrence of the duct rupture accident, the steady convection can form. In fact, the initial lower core temperature distribution cannot provide enough propelling tendency to form steady convection in such a short time. 32.78 hours is a conservative onset time for steady convection.

The axis of improvement for future researches shall focus on finding accurate diffusion coefficients for more than two gases diffusion processes and on using a time-dependent temperature field in replacement of the constant one. The DIFFLOW code can calculate one-dimensional models so far. Some research methods using commercial software have become popular in recent years, for example CFD. [7] Three-dimensional models could be set up in convenient ways.

Nomenclature

A: Cross section area of the channel
C: Total molar concentration
C_f: Frictional resistance coefficient
c_p: Constant-pressure specific heat capacity
D_H: Equivalent diameter
D_i: The effective diffusion coefficient of species i
K: Local resistance coefficient
K_i: Sum of all evaluation values on level i
$\overline{K}_i$: Mean of all evaluation values on level i
p: relative gas pressure
p_a: Atmosphere pressure
q_{eff}: Equivalent inner heat source
R: Range of means
T: Gas temperature
T_W: Temperature of channel wall
T_∞: Temperature of gas in cavity
u: Velocity
x_i: Mole fraction of species i in a mixture
x_i^0: Initial x_i in reactor passage
x_i^∞: Initial x_i in cavity
α: surface coefficient of heat transfer
λ: Heat conductivity
ρ: Density
ξ: 1 for up flow, 0 for horizontal flow, -1 for down flow
μ: Dynamic viscosity

Acknowledgement

This work has been supported by the National S&T Major Project (Grant No. ZX06901).

References

[1] ZHANG, Z., WU, Z., WANG, D., XU, Y., SUN, Y., LI, F., and DONG, Y.: Current Status and Technical Description of Chinese 2×250MWth HTR-PM Demonstration Plant, Nuclear Engineering and Design, 2009, 239:1212-1219.

[2] LIU, B.: Study on Air Ingress Accident of 10MW High Temperature Gas-cooled Test Reactor, Beijing: Tsinghua University, 1998.

[3] TAKEDA, T, and HISHIDA, M.: Studies on Diffusion and Natural Convection of the Two Component Gases. In: Proceeding of the International Topical Meeting on the Safety, Status and Future of Non-commercial Reactors and Irradiation Facilities, 1990.

[4] ZHANG, Z, GERWIN, H, and SCHERER, W.: Analysis of the Gas-Diffusion Process during a Hypothetical Air Ingress Accident in a Modular High Temperature Gas Cooled Reactor, Julich: Institue fur Sicherheitsforschung und Reaktortechnik, 1993.

[5] ZHENG, Y., and SHI, L.: Characters of the 250MW Pebble-Bed Modular High Temperature Gas-Cooled Reactor in Depressurized Loss of Coolant Accidents. In: 4th International Topical Meeting on High Temperature Reactor Technology (Proceedings HTR2008), 2008.

[6] ZHENG, Y, SHI, L, and DONG, Y.: Thermohydraulic Transient Studies of the Chinese 200 MWe HTR-PM for Loss of Forced Cooling Accidents, Annals of Nuclear Energy, 2009, 36(6): 742-751.

[7] SCHMITZ, W., and KOSTER, A.: Air Ingress Simulations Using CFD. In: 3rd International Topical Meeting on High Temperature Reactor Technology (Proceedings HTR2006), 2006.